Research Article

Nano-Liposomal Encapsulation-Delivered Apelin-13 Attenuates Ev71 Infection-Induced Neurodegeneration by Modulating Il-6 and Tlr7

Shengnan Xu[1], Cheng Cui[1], Manchao Sun[1], Sihui Guo[1], Ke Xu[1], Yanan Cui[1], Ziyin Gao[1], Zhenqi Wu[1], Jiaxin Xue[1], Yucai Ma[1], Xue He[1], Guofeng Cai[2*]

[1]Hospital of Heilongjiang University of Traditional Chinese Medicine, Harbin, Heilongjiang Province, China

[2]Hanan Branch of Second Affiliated Hospital of Heilongjiang University of Traditional Chinese Medicine, Harbin, Heilongjiang Province, China

*Correspondence to: Guofeng Cai, PhD, Associate Chief Physician, Internal Medicine, Hanan Branch of Second Affiliated Hospital of Heilongjiang University of Traditional Chinese Medicine, Hanan 2nd Avenue, Harbin 150060, China; Email: wulongels@163.com

Abstract

Background: Enterovirus 71 (EV71) infection serves as a leading cause of hand-foot-and-mouth disease, and induces neural disorders. Apelin-13, as a neuropeptide, presents potential neuroprotective activities, but its short half-life in circulation has limited its clinical use.

Objective: To explore the role of nano-liposomal encapsulation-delivered apelin-13 in the development of EV71 infection-induced neurodegeneration.

Method: The liposome encapsulating apelin-13 (lipoPEG-A13) was successfully constructed and characterized in the study. The neurodegeneration measurement in an intracranially EV71-infected mouse model was performed *in vivo*. MTT assays, lactate dehydrogenase release assays, immunohistochemistry, and immunofluorescence staining qPCR assays, and Western blot analysis were respectively performed.

Results: EV71 notably replicated and promoted apoptosis in the cerebral cortex from the EV71-infected mice but exhibited comparatively low replication and slightly regulated apoptosis in the cerebellum. Remarkably, lipoPEG-A13 was able to inhibit EV71-induced neurological injury in the murine cerebral cortex *in vivo*. Meanwhile, LipoPEG-A13 could attenuate EV71-caused apoptosis of the neural cell in the brain. LipoPEG-A13 decreased the Toll-like receptor 7 (TLR7) and interleukin-6 (IL-6) production in the mice. Apelin-13 inhibited the expression of TLR7 and IL-6 in the human astroglioma U251 cells. Apelin-13 could reduce the apoptosis of astrocytic cells infected with EV71.

Conclusion: Nano-liposomal encapsulation-delivered apelin-13 attenuated EV71 infection-induced neurodegeneration via modulating IL-6 and TLR7 production. The finding provides new insights into how Nano-liposomal encapsulation-delivered apelin-13 modulates EV71 infection-induced neurological disorders. The Nano-liposomal encapsulation-delivered apelin-13 presents the application potential in the clinical context.

1 INTRODUCTION

Enterovirus 71 (EV71) serves as an RNA virus and is a principal contributor to the hand-foot-and-mouth disease, regularly producing the tempered symptom in infants, but causing severe disorders, such as acute flaccid paralysis, brain stem encephalitis, and aseptic meningitis[1-4]. The increasing EV71-induced outbreak has been the case of significant public health matter and is accountable for extended mortality and neurovirulence, especially in the Asian-Pacific region[5-7]. EV71 infection induces severe neurological disease with well-defined clinic radiological symptoms in related patients, leading to a more considerable paresis-associated incidence in the spinal cord or brainstem[8]. The progression of EV71 infection-related neurodegeneration involves multiple inflammatory factors, such as Toll-like receptor 7 (TLR7) and interleukin-6 (IL-6)[9]. TLR7 and IL-6 play crucial roles in neurodegeneration. Exploring the therapeutic candidate for the EV71 infection-induced neurological symptoms is hugely needed.

Apelin is a neuropeptide obtained from stolid abdomen tissues and sustains cleaved from apelin-36, apelin-17, and apelin-13[10]. Apelin-13 serves as a more effective type of apelin in competing for interacting with the APJ[11]. The distribution of apelin-13 in the hypothalamus, substantia nigra, striatum, cerebellum, hippocampus, hypothalamus, and amygdala, implies that apelin-13 may display crucial and broad functions in pathophysiological and physiological processes[12]. It has been identified that the apelin-13/APJ system may play a critical function in the neuronal protection and pathway in the central neuronal system[13].

Broadly clinic apelin-13 application is severely hindered by the peptide's unstable feature in both *in vivo* and in vitro situations[14,15]. The plasma variability of apelin-13 is owed to the fast degeneration[16,17], which leads to a remarkably short half-life (<8min) in plasma[18]. Nanoparticle drug formulation has been identified to be beneficial for the continued transfer of therapeutic agents in numerous disorders[19,20]. Amidst a type of Nanoparticle, the liposome is generally regarded as a proper vesicle for potentially targeted drug transmission[21]. The liposome peptide delivery system caters to different physiological requirements[22]. To improve drug targeting efficiency, the ligand for the receptor of the individual cell surface requires to be organized into Nanoparticles[22]. Liposome encapsulation of drugs can achieve this use by employing various loading methods[21]. Acknowledging that facade alteration of liposomes can increase the drug deliverance characteristics of Nanoparticles, a substantial number of investigations focus on the liposome-drug interaction[23]. However, the effect of Nano-liposomal encapsulation-delivered apelin-13 on the progression of EV71 infection-induced neurodegeneration is still obscure.

We identified a novel neuroprotective function of nano-liposomal encapsulation-delivered apelin-13 in the EV71 infection-induced neurodegeneration via modulating TLR7 and IL-6 production.

2 MATERIALS AND METHODS

2.1 Liposome Encapsulation and Characterization

Lipids utilized to construct the liposomes contain 1,2-distearoyl-sn-glycero-3- phosphocholine (DSPC) (Avanti polar lipids, Inc., USA), cholesterol (Sigma, USA), and 1,2-distearoyl-sn-glycero-3-phosphoethanolamine-N-[amino (polyethylene glycol)-3400] (DSPE-PEG(3400)-NH2) (Laysa, China) . PEG-carrying liposome (lipo-PEG) was equipped by dissolving NH2-PEG-DSPE (2mg), DSPC (10mg), and cholesterol (5mg) in chloroform (1mL). The mix-up was concentrated following a vacuum condition in a rotary evaporator to produce a thin sheet of particles. The lipid layers were hydrated by the double-distilled water and sonicated (30min) to get a turbid liposome solution. The solutions were cooled and lyophilized to get solvent-free dry liposomes. Apelin-13 was encapsulated by hydrating the liposomes (17mg) with apelin-13 (3.3mg) in the double-distilled water (1mL) followed by 30min sonication. The characterization of the Nanoparticles was analyzed by atomic force microscopy (AFM) and dynamic light scattering measurements.

2.2 Animal Investigation

The C57BL/6 mice (three-day-old) were obtained (Shanghai Laboratory Animal Center) and were intracranially injected with PBS (10μL) containing EV71 1×10^9 plaque-forming units (PFU)/mL using gastight microsyringe (50μL, Hamilton, USA). After EV71 infection, mice's clinical score and weight were registered each day till one-week after treatment. The whole spine of the mice was discarded to obtain CSF. The CSF (10μL) was aspirated by micro syringe and thinned in PBS (1mL). The IL-6 protein expression was analyzed by ELISA assays (4A Biotech Co. Ltd; Beijing, China). The EV71 RNA copies were measured by qPCR assays. The cleaved caspase-3 (cl-caspase-3) was analyzed by fluorescence staining in

the cerebral cerebellum. The levels of neurofilaments were determined by fluorescence staining in the cortex of the mice. The levels of EV71 dsRNA were analyzed by IHC staining in the cerebral cortex of the mice. The neurodegeneration of the cerebral cortex in the mice was analyzed by Hematoxylin and Eosin (HE) staining in the mice. The Animal Ethics Committee authorized animal care and method procedure. The animal study was reviewed and approved by Hospital of Heilongjiang University of Traditional Chinese Medicine.

2.3 EV71 Infection

The EV71 virus (Xiangyang-Hubei-09) was obtained in a one-year-old dead infant's brain tissue infected with EV71 and previously isolated (GenBank accession no. JN230523.1). Propagated EV71 in RD cells. EV71 titration and inoculation were conducted as previously reported[24,25]. Aliquots were deposited at -80°C before further analysis. The EV71 at indicated multiplicities of infection (MOIs) was used to infect U251 cells, after which the cells were cultured at 37°C for an additional 24h or 48h.

2.4 Terminal Deoxynucleotidyl Transferase Dutp Nick End Labeling (TUNEL)

The TUNEL detection kit (Roche, Germany) was used to analyze apoptosis in the mice according to the product's guidance. After the staining of TUNEL, the ventricular samples were dyed by DAPI (Sigma, USA) to stain nuclear. Fluorescence was observed using a confocal microscope (Olympus Fluoview1000, Tokyo, Japan).

2.5 Cell Culture and Treatment

The astroglioma U251 cells was obtained from American Type Tissue Culture Collection. The cells were cultured in the medium of DMEM (Gibco, USA) containing 0.1mg/ml streptomycin (Gibco, USA), 100units/ml penicillin (Gibco, USA), and 10% fetal bovine serum (Gibco, USA), at a condition of 37°C with 5% CO_2. The cells were treated with apelin-13 (10^{-9} mol/L, Santa Cruz, USA).

2.6 MTT Assays

MTT assays measured the cell viability of U251 cells. Briefly, about 1×10^4 U251 cells were put into 96 wells and cultured for 12h. After treatment, the cells were added with a 10μL MTT solution (5mg/mL) (Sigma, USA) and cultured for an extra 4h. Discarded medium, and 150μL/well DMSO (Thermo, USA) was used to treat the wells. An ELISA browser was applied to analyze the absorbance at 570nm (Bio-Tek EL 800, USA).

2.7 Lactate Dehydrogenase (LDH) Release Assays

Cell injury was analzyed by estimating the LDH utilizing an LDH detection kit (Dojindo, Japan) according to the manufacturer's instructions. Shortly, the mediums were collected from 24-well plates and centrifuged (5000rpm, 10min). Then, the supernatants were incubated with the provided reaction mixture, and LDH activities were measured at 450nm absorbance.

2.8 Quantitative Reverse Transcription-PCR (qRT-PCR)

The total RNAs were extracted by TRIZOL (Invitrogen, USA) from the tissues and cells. The first-strand cDNA was synthesized using Stand cDNA Synthesis Kit (Thermo, USA) as the manufacturer's instruction. The qRT-PCR was carried out by applying SYBR RT-PCR kit (Roche, USA). The standard control for mRNA was GAPDH. Quantitative determination of the RNA levels was conducted by SYBR GreenPremix Ex TaqTM II Kit (TaKaRa, Japan). The experiments were independently repeated at least three times. The primer sequences are as follows:

Mouse TLR7 forward: 5′-GTTCTATGGAGAGCCGGTGATA-3′
Mouse TLR7 reverse: 5′-ATTCTTTAGATTTGGCGGCATA-3′
Mouse IL-6 forward:5′-AGACAAAGCCAGAGTCCTTCAGAGA-3′
Mouse IL-6 reverse: 5′-GCCACTCCTTCTGTGACTCCAGC-3′
Mouse IL-1β forward: 5′-AGCTTCAGGCAGGCAGTATC-3′
Mouse IL-1β reverse: 5′-CGTCACACACCAGCAGGTTA-3′
Mouse Cxcl-1 forward: 5′-CTTGAAGGTGTTGCCCTCAG-3′
Mouse Cxcl-1reverse: 5′-TGGGGACACCTTTTAGCATC-3′
Mouse TNFα forward: 5′-ACGTGGAACTGGCAGAAGAG-3′
Mouse TNFα reverse: 5′-CTCCTCCACTTGGTGGTTTG-3′
Mouse GAPDH forward: 5′-ATGTTTGTGATGGGTGTGAA-3′
Mouse GAPDH reverse: 5′-ATGCCAAAGTTGTCATGGAT-3′
Mouse Caspase3 forward: 5′-TGGTGATGAAGGGGTCATTTATG-3′
Mouse Caspase3 reverse: 5′-TTCGGCTTTCCAGTCAGACTC-3′
EV71 VP1 forward: 5′-GAGTTCCATAGGTGACAGC-3′
EV71 VP1 reverse: 5′-CTGTGCGAATTAAGGACAG-3′
Human TLR7 forward: 5′-TTTACCTGGATGGAAACCAGCTA-3′
Human TLR7 reverse: 5′-TCAAGGCCTGAGAAGCTGTAAGCTA-3′
Human IL-6 forward: 5′-GTACATCCTCGACGGCATCTCA-3′
Human IL-6 reverse: 5′-GCACAGCTCTGGCTTGTTCCTC-3′
GAPDH forward: 5′-AGAAGGCTGGGGCTCATTTG-3′.
GAPDH reverse: 5′-AGGGGCCATCCACAGTCTTC-3′

2.9 Western Blot Analysis

Total proteins were extracted from the rats and cells with RIPA buffer (CST, USA). Protein concentrations were measured by using the BCA Protein Quantification Kit (Abbkine, USA). Same concentration of protein was divided by SDS-PAGE (12% polyacrylamide gels), transferred to PVDF membranes (Millipore, USA) in the subsequent step. The membranes were hindered with 5% milk and hatched overnight at 4°C with the primary antibodies for PARP (Abcam, USA), caspase-3 (Abcam, USA), VP1 (Abcam, USA), and β-actin (Abcam, USA), in which β-actin served as the control. Then, the corresponding second antibodies (1:1000) (Abcam, UK) were used for hatching the membranes 1h at room temperature, followed by the visualization by using an Odyssey CLx Infrared Imaging System. The results of Western blot analysis were quantified by ImageJ software.

2.10 Statistical Analysis

Data were presented as mean ± SD, and the statistical analysis was performed by GraphPad prism 7. The unpaired Student's t-test was applied for comparing two groups, and the one-way ANOVA was applied for comparing among multiple groups. $P<0.05$ were considered as statistically significant.

3 RESULTS

3.1 The Characterization of Liposome Encapsulating Apelin-13 (lipoPEG-A13)

The lipoPEG-A13 was constructed and characterized. The PEG liposomes topography maps were generated by the AFM. Our data showed that the dynamic light scattering (DLS) was applied to analyze the size distribution of the empty PEG-liposomes and PEG-liposomes encapsulated with apelin-13, in the presence or absence of 0.5% BSA (Figure 1A). The average size of the empty PEG-liposomes was about 0.56±0.02 (SD) mm. In the presence of 0.5% BSA, there was nearly no difference in size (0.53±0.02 (SD) mm) for empty PEG-liposome particles. But lipoPEG-A13 showed a remarkable decrease in particle size to 0.05±0.00mm. The presence of 0.5% BSA in the particles of lipoPEG-A13 improved their size to 0.24±0.02 (SD) mm. LipoPEG-A13 demonstrated maintained and prolonged drug release when monitored over a 24h period at different time intervals and physiological conditions *in vitro* (Figure 1B and 1C).

3.2 The Neuropathogenesis Assessment in Intracranially Ev71-Infected Mice

Then, to assess whether EV71 infection caused neuro disorder in the brain of mice, the mice were intracranially injected with PBS or EV71. Our data showed the apoptosis of neural cells in the mice. We observed lower levels of dsRNA and cl-Caspase-3 in the cerebellum compared to the cerebral cortex of EV71-infected mice on day one post-infection (Figure 2A and 2B). Together these data suggest that EV71 could remarkably replicate and induce apoptosis in the cerebral cortex of EV71-infected mice.

3.3 LipoPEG-A13 Inhibits EV71-induced Neural Pathogenesis in the Murine Cerebral Cortex

Next, we analyzed the role of lipoPEG-A13 in the EV71 infection and replication. Notably, IHC staining showed that lipoPEG-A13 was not able to affect the levels of EV71 dsRNA in the cerebral cortex of the mice (Figure 3A), suggesting that lipoPEG-A13 cannot affect EV71 infection and replication. Then, the effect of lipoPEG-A13 on the EV71 infection-induced neuropathogenesis in the mice. Significantly, the mice treated with lipoPEG-A13 presented a higher body weight, lower clinical scores, and higher survival rates (Figure 3B-3D). Together these data indicate that lipoPEG-A13 is able to inhibit EV71-induced neural pathogenesis.

3.4 LipoPEG-A13 Attenuates EV71-induced Neural Cell Apoptosis in the Brain

Given that the EV71 infection-induced neuro disorder is commonly correlated with neural cell apoptosis, we tried to assess the function of lipoPEG-A13 in modulating EV71 infection-induced neural cell apoptosis. It has been reported that the neuroinflammation response plays a crucial role in the modulation of neural injury[26]. Western blotting further confirmed that the treatment of lipoPEG-A13 reduced cleaved-caspase-3 in the cerebral cortex of the mice (Figure 4A and 4B). Moreover, the TUNEL positive cells were decreased by lipoPEG-A13 treatment in the mice (Figure 4C). Together these data suggest that lipoPEG-A13 attenuates EV71-induced neural cell apoptosis *in vivo*.

3.5 Apelin-13 Inhibits TLR7 and IL-6 Production *in Vivo* and *in Vitro*

Next, we further investigated the underlying mechanism of lipoPEG-A13-regulated neural pathogenesis induced by the EV71 infection. Given that TLR7 and IL-6 are involved in the EV71 infection-induced neurodegeneration, we tried to explore whether lipoPEG-A13 exerted its neural protection effect by modulating TLR7 and IL-6. Significantly, the expression of TLR7 and IL-6 was reduced by the treatment of lipoPEG-A13 (Figure 5A and 5B). Meanwhile, the treatment of apelin-13 was able to decrease the expression of TLR7, IL-6, and IL-8, but not TNF-α, in the EV71-infected human astroglioma U251 cells (Figure 6A-6E). Together these data suggest that apelin-13 can inhibit the production of TLR7 and IL-6 *in vivo* and *in vitro*.

3.6 Apelin-13 Attenuates Astrocytic Cell Apoptosis upon EV71 Infection in U251 Cells

Then, we evaluated the effect of apelin-13 on the EV71 infection-related astrocytic cell injury *in vitro*. MTT assays showed that the treatment of apelin-13 enhanced cell viability in the EV71-infected human astroglioma U251 cells (Figure 7A). The LDH release was reduced by the
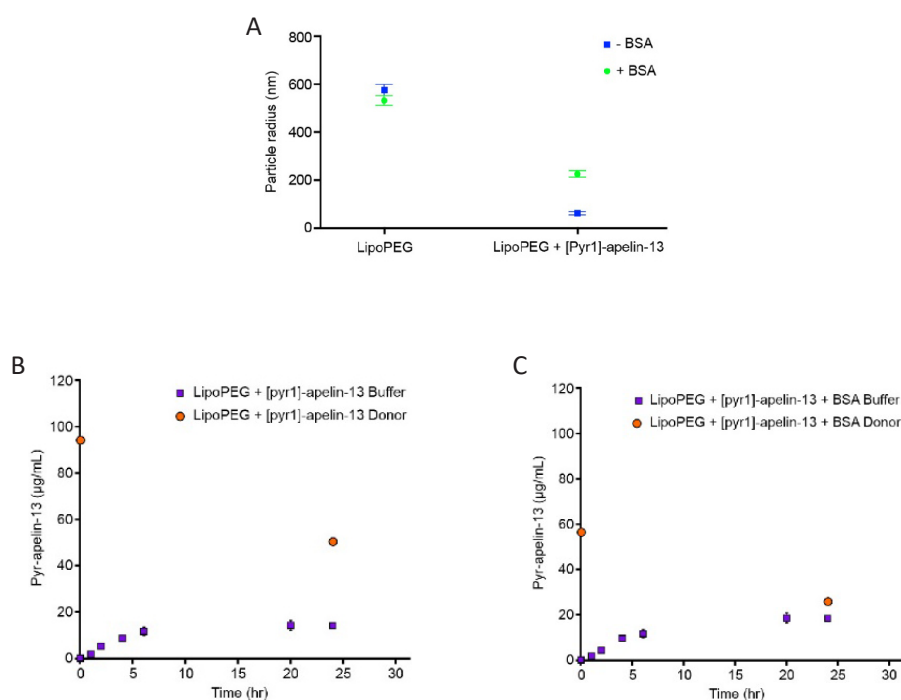
Figure 1. The characterization of liposome encapsulating apelin-13. A: The size distribution of the PEG liposome particles and the particles of PEG liposome-apelin-13 was analyzed by DLS; B and C: The drug release was performed by time course analysis.
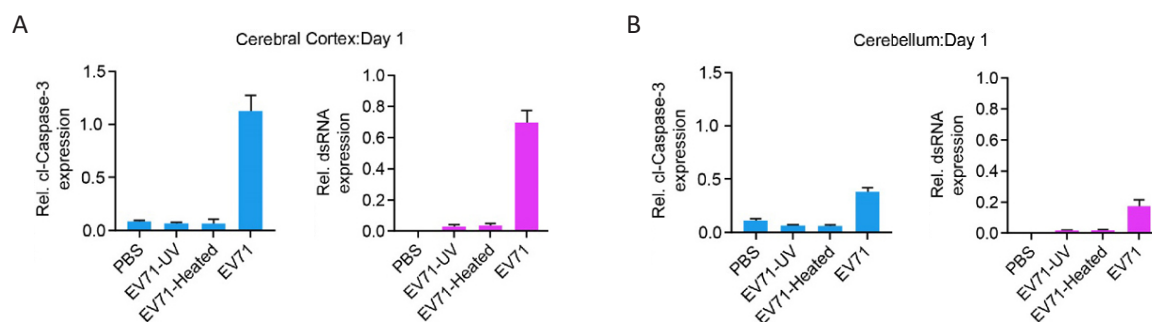

Figure 2. The neuropathogenesis assessment in intracranially EV71-infected mice. A and B: The expression of cl-caspase-3 was analyzed by fluorescence staining in the cerebral cerebellum of mice. The relative expression of cl-caspase-3 and dsRNA was quantified using Image J software. Data are presented as mean ± SD.

treatment of apelin-13 in the cells (Figure 7B), indicating that apelin-13 can attenuate EV71 infection-induced cell injury. Moreover, the treatment of apelin-13 could reduce the EV71 infection-promoted expression of cl-caspase-3 and cleaved PARP (cl-PARP) in the cells (Figure 7C), suggesting that apelin-13 attenuates EV71-infected astrocytic cell apoptosis.

4 DISCUSSION

As a neuropeptide, several roles of apelin-13 in the modulation of PD development have been reported. The previous study has identified that apelin-13 plays a critical function in the neuronal protection and modulation of the central neuronal system. It has been identified that apelin-13 relieves ER stress-regulated neural apoptosis by stimulating Gα i/Gα q-CK2 axis[27]. Apelin-13 reduces initial brain damage of subarachnoid hemorrhage by repressing neural apoptosis through the GLP-1R/PI3K/Akt pathway[28]. Apelin-13 inhibits neuroinflammation upon cognitive deficiency by activating the brain-derived neurotropic factors (BDNF)/TrkB signaling[29]. Apelin-13 preserves the neurovascular system upon ischemic damage by affecting vascular endothelial growth factors[30]. Apelin guards upon NMDA-produced retinal neural loss through the APJ receptor by stimulating ERK1/2 and Akt and containing TNF-α production *in vivo*[31]. Meanwhile, the Nano delivery system has been applied to neuronal protection. For example, it has been identified that Nano-liposome-lycopene decreases ischemic brain injury by modulating iron metabolism in rodents[32]. Nano sterically steadied liposomes for the treatment of neurodegenerative inflammation disorders have been reported[33]. Targeted BDNF transmission using magnetic Nanocarriers across the blood-brain barrier for neuroprotection have been
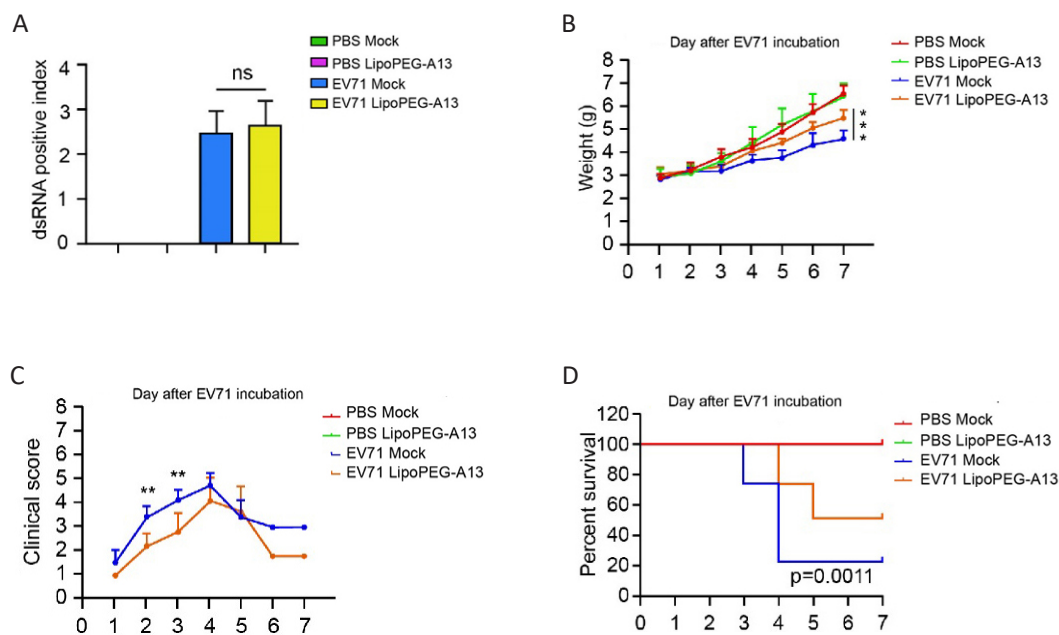
Figure 3. LipoPEG-A13 inhibits EV71-induced neural pathogenesis in the murine cerebral cortex. A: The levels of EV71 dsRNA in the cerebral cortex of the mice were analyzed by IHC staining; B to D: The body weight, clinical scores, and survival rates were assessed in the mice. Data are presented as mean ± SD. Statistic significant differences were indicated: **$P<0.01$; ns, no significance.
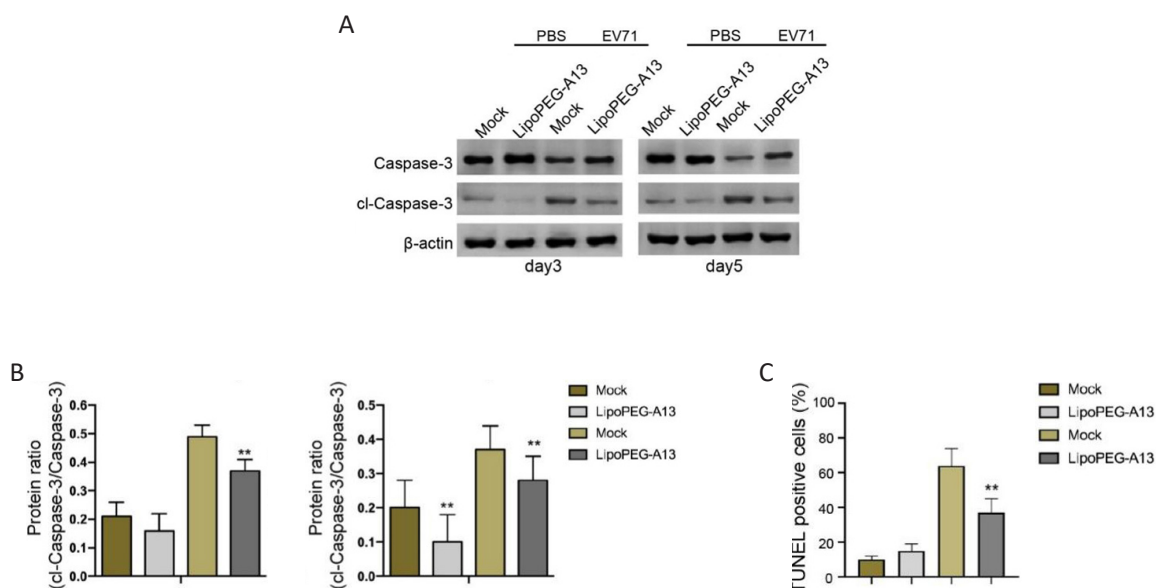

Figure 4. LipoPEG-A13 attenuates EV71-induced neural cell apoptosis in the brain. A and B: The expression of caspase-3, cl-caspase-3, and β-actin was measured by Western blot analysis in the mice; C: The apoptosis was analyzed by TUNEL analysis in the mice. Data are presented as mean ± SD. Statistic significant differences were indicated: **$P<0.01$.

identified[34]. In this study, the liposome encapsulating lipoPEG-A13 was successfully constructed and characterized, conjugated with PEG polymer on their surface. lipoPEG-PA13 was able to inhibit EV71-produced neural injury in the murine cerebral cortex. Meanwhile, lipoPEG-A13 could attenuate EV71-induced apoptosis of neural cells from the brain. These data innovatively development the Nano-liposomal encapsulation-delivered system of apelin-13 in the inhibition of V71 infection-induced neurodegeneration, providing valuable evidence of the application of Nano-liposomal delivery system and

apelin-13 in neuronal protection. Interestingly, we showed the expression of c-caspase and ds RNA upon viral insult in the cortex and cells expressing these markers appear very small, in which the cell types should be explored and identified in future investigations.

Toll-like receptors (TLRs) are innate immune receptors and identify pathogen-related particles of specific immune cells[35]. Different TLRs are dispatched in microglial cells, astrocytes, and neurons, and TLRs are favorable to the immune response of the central nervous system (CNS)[36].
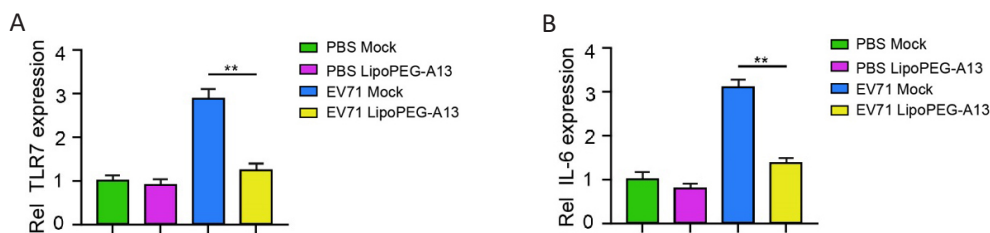
Figure 5. LipoPEG-A13 inhibits TLR7 and IL-6 production *in vivo*. A and B: The C57BL/6 WT mice were intracranially injected with EV71 and treated with lipoPEG-A13. The expression of TLR7 and IL-6 was measured by qPCR assays in the mice. Data are presented as mean ± SD. Statistic significant differences were indicated: **$P<0.01$.
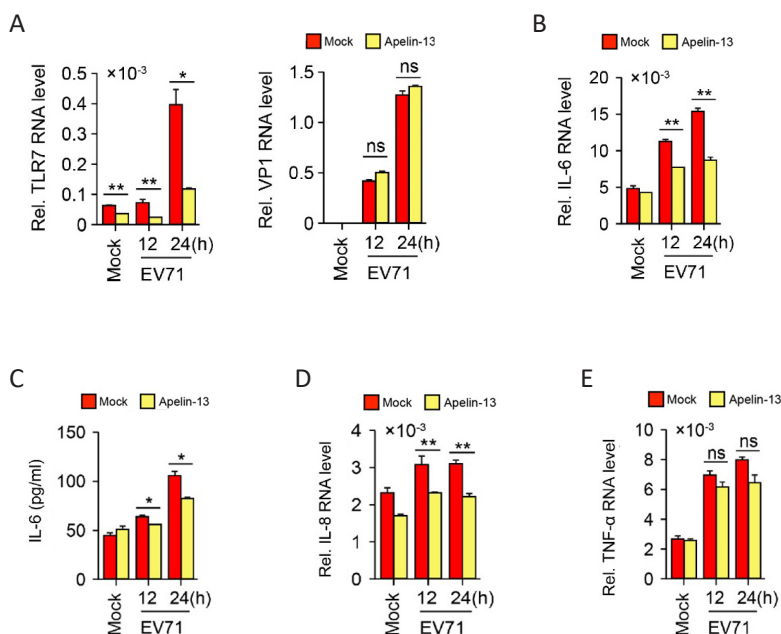

Figure 6. Apelin-13 inhibits TLR7 and IL-6 production *in vitro*. A-E: The human astroglioma U251 cells were injected with EV71 and treated with apelin-13; A and B: The expression of TLR7 and IL-6 was measured by qPCR assays in the cells; C: The production of IL-6 in the culture medium was analyzed by ELISA assays in the cells; D and E: the expression of IL-8 and TNF-α was assessed by qPCR assays in the cells. Data are presented as mean ± SD. Statistic significant differences were indicated: *$P<0.05$; **$P<0.01$; ns, no significance.

Increasing evidence indicates that TLRs perform a crucial function in the brain's homeostasis regulation[37]. TLR7 is generally expressed in neural, lung, intestinal, and immune cells, which are detected and responded to particular microRNAs, siRNAs, single-stranded oligoribonucleotides, and viral RNA, causing cytokine production and intracellular signaling activation[38]. In several sorts of non-infected CNS damage, TLR7 works as a notable regulator of neuropathogenesis[39]. TLR7 is able to thus perform extensive regulatory functions in a range of signaling regarding cell biology, innate immunity, and neurodegeneration[40]. Besides, it has been reported that IL-6 is abnormally expressed in the EV71-infected mice and participates in the modulation of neurodegeneration[41,42]. EV71 infection causes neurodegeneration through the activation of TLR7 signaling and IL-6 expression[9]. Here, we identified that lipoPEG-A13 decreased TLR7 and IL-6 production in the mice. Apelin-13 inhibited the expression of TLR7 and IL-6 in the U251 cells. These data demonstrate the unreported effect of Nano-liposomal

encapsulation-delivered system of apelin-13 on the TLR7 and IL-6 in the EV71 infection-induced neurodegeneration. There are still some limitations in the current study. For example, TLR7 and IL-6 are just one of the downstream factors under nano-liposomal encapsulation-delivered apelin-13-regulated neurodegeneration and other potential mechanisms should be explored in future investigations. Meanwhile, the clinical significance of nano-liposomal encapsulation-delivered apelin-13 should be confirmed in the future.

5 CONCLUSION

In conclusion, we discovered that nano-liposomal encapsulation-delivered apelin-13 attenuated EV71 induced neurodegeneration by modulating IL-6 and TLR7. Our finding provides new insights into the mechanism by which Nano-liposomal encapsulation-delivered apelin-13 modulates EV71 infection-induced neurological disorders. The Nano-liposomal encapsulation-delivered apelin-13 presents the application potential in the clinical context.
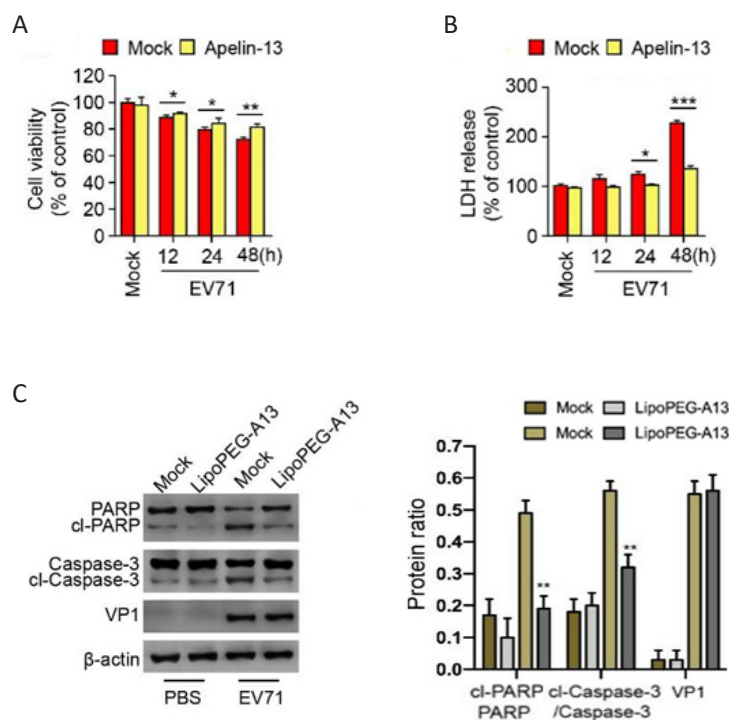
Figure 7. Apelin-13 attenuates astrocytic cell apoptosis upon EV71 infection in U251 cells. A-C: The human astroglioma U251 cells were injected with EV71 and treated with apelin-13; A: The cell viability was analyzed by MTT assays in the cells; B: The cell injury was measured by LDH analysis in the cells; C: The expression of caspase-3, cleaved-caspase-3, PARP, cleaved-PARP, VP1, and β-actin was tested by Western blot analysis in the cells. Data are presented as mean ± SD. Statistic significant differences were indicated: *$P<0.05$; **$P<0.01$; ***$P<0.001$.

Conflicts of Interest
These authors declared no conflict of interest.

Author Contribution
Xu S, Cui C and Sun M performed the majority of experiments and analyzed the data. Guo S and Xu K performed the molecular investigations. Cui Y, Gao Z and Wu Z designed and coordinated the research. Xue J, He X, Cai G and Ma Y wrote the paper.

Abbreviation List
AFM, Atomic force microscopy
cl-caspase-3, Cleaved caspase-3
cl-PARP, Cleaved PARP
CNS, Central nervous system
EV71, Enterovirus 71
IL-6, Interleukin-6
LDH, Lactate dehydrogenase
lipoPEG-A13, Liposome encapsulating apelin-13
PFU, Plaque-forming units
TLR7, Toll-like receptor 7
TLRs, Toll-like receptors

References
[1] Zhu J, Chen N, Zhou S et al. Severity of enterovirus A71 infection in a human SCARB2 knock-in mouse model is dependent on infectious strain and route. *Emerg Microbes Infect*, 2018; 7: 1-13. DOI: 10.1038/s41426-018-0201-3.

[2] Xu Y, Ma S, Zhu L et al. Clinically isolated enterovirus A71 subgenogroup C4 strain with lethal pathogenicity in 14-day-old mice and the application as an EV-A71 mouse infection model. *Antiviral Res*, 2017; 137: 67-75. DOI: 10.1016/j.antiviral.2016.11.008.

[3] Hu Y, Jiang L, Peng HL. Clinical analysis of 134 children with nervous system damage caused by enterovirus 71 infection. *Pediatr Infect Dis J*, 2015; 34: 718-723. DOI: 10.1097/INF.0000000000000711.

[4] Huang PN, Shih SR. Update on enterovirus 71 infection. *Curr Opin Virol*, 2014; 5: 98-104. DOI: 10.1016/j.coviro.2014.03.007.

[5] Solomon T, Lewthwaite P, Perera D et al. Virology, epidemiology, pathogenesis, and control of enterovirus 71. *Lancet Infect Dis*, 2010; 10: 778-90. DOI: 10.1016/S1473-3099(10)70194-8.

[6] Xing W, Liao Q, Viboud C et al. Hand, foot, and mouth disease

in China, 2008-12: an epidemiological study. *Lancet Infect Dis*, 2014; 14: 308-318. DOI: 10.1016/S1473-3099(13)70342-6.

[7] Zhang Y, Zhu Z, Yang W et al. An emerging recombinant human enterovirus 71 responsible for the 2008 outbreak of hand foot and mouth disease in Fuyang city of China. *Virol J*, 2010; 7: 94. DOI: 10.1186/1743-422X-7-94.

[8] Teoh HL, Mohammad SS, Britton PN et al. Clinical characteristics and functional motor outcomes of enterovirus 71 neurological disease in children. *JAMA Neurol*, 2016; 73: 300-307. DOI: 10.1001/jamaneurol.2015.4388.

[9] Luo Z, Su R, Wang W et al. EV71 infection induces neurodegeneration via activating TLR7 signaling and IL-6 production. *PLoS Pathog*, 2019; 15: e1008142. DOI: 10.1371/journal.ppat.1008142.

[10] Antushevich H, Wojcik M. Apelin in disease. *Clin Chim Acta*, 2018; 483: 241-8. DOI: 10.1016/j.cca.2018.05.012.

[11] Mughal A, O'Rourke ST. Vascular effects of apelin: Mechanisms and therapeutic potential. *Pharmacol Ther*, 2018; 190: 139-47. DOI: 10.1016/j.pharmthera.2018.05.013.

[12] Kurowska P, Barbe A, Różycka M et al. Apelin in reproductive physiology and pathology of different species: a critical review. *Int J Endocrinol*, 2018; 2018: 9170480. DOI: 10.1155/2018/9170480.

[13] Zhang X, Peng X, Fang M et al. Up-regulation of apelin in brain tissue of patients with epilepsy and an epileptic rat model. *Peptides*, 2011; 32: 1793-9. DOI: 10.1016/j.peptides.2011.08.006.

[14] Andersen CU, Hilberg O, Mellemkjaer S et al. Apelin and pulmonary hypertension. *Pulm Circ*, 2011; 1: 334-346. DOI: 10.4103/2045-8932.87299.

[15] Tamargo J, Duarte J, Caballero R et al. New therapeutic targets for the development of positive inotropic agents. *Discov Med*, 2011; 12: 381-392.

[16] Murza A, Belleville K, Longpre JM et al. Stability and degradation patterns of chemically modified analogs of apelin-13 in plasma and cerebrospinal fluid. *Peptide Sci*, 2014; 102: 297-303. DOI: 10.1002/bip.22498.

[17] Mesmin C, Renvoise M, Becher F et al. MS-based approaches to unravel the molecular complexity of proprotein-derived biomarkers and support their quantification: the examples of B-type natriuretic peptide and apelin peptides. Bioanalysis, 2012; 4: 2851-63. DOI: 10.4155/bio.12.259.

[18] Japp AG, Cruden NL, Amer DAB et al. Vascular effects of apelin *in vivo* in man. *J Am Coll Cardiol*, 2008; 52: 908-913. DOI: 10.1016/j.jacc.2008.06.013.

[19] Donaldson K, Duffin R, Langrish JP et al. Nanoparticles and the cardiovascular system: a critical review. *Nanomedicine*, 2013; 8: 403-23. DOI: 10.2217/nnm.13.16.

[20] Brito L, Amiji M. Nanoparticulate carriers for the treatment of coronary restenosis. *Int J Nanomed*, 2007; 2: 143-61.

[21] Allen TM, Cullis PR. Liposomal drug delivery systems: from concept to clinical applications. *Adv Drug Deliv Rev*, 2013; 65: 36-48. DOI: 10.1016/j.addr.2012.09.037.

[22] Kumar P, Gulbake A, Jain SK. Liposomes a vesicular nanocarrier: potential advancements in cancer chemotherapy. *Crit Rev Ther Drug*, 2012; 29: 355-419. DOI: 10.1615/

CritRevTherDrugCarrierSyst.v29.i5.10.

[23] Chen Z, Deng J, Zhao Y et al. Cyclic RGD peptide-modified liposomal drug delivery system: enhanced cellular uptake in vitro and improved pharmacokinetics in rats. *Int J Nanomed*, 2012; 7: 3803. DOI: 10.2147/IJN.S33541.

[24] Ge M, Luo Z, Qiao Z et al. HERP binds TBK1 To activate innate immunity and repress virus replication in response to endoplasmic reticulum stress. *J Immunol*, 2017; 199: 3280-3292. DOI: 10.4049/jimmunol.1700376.

[25] Luo Z, Dong X, Li Y et al. PolyC-binding protein 1 interacts with 5'-untranslated region of enterovirus 71 RNA in membrane-associated complex to facilitate viral replication. *PLoS One*, 2014; 9: e87491. DOI: 10.1371/journal.pone.0087491.

[26] Berger M, Ponnusamy V, Greene N et al. The effect of propofol vs. isoflurane anesthesia on postoperative changes in cerebrospinal fluid cytokine levels: results from a randomized trial. *Front Immunol*, 2017; 8: 1528. DOI: 10.3389/fimmu.2017.01528.

[27] Wu F, Qiu J, Fan Y et al. Apelin-13 attenuates ER stress-mediated neuronal apoptosis by activating Galphai/Galphaq-CK2 signaling in ischemic stroke. *Exp Neurol*, 2018; 302: 136-44. DOI: 10.1016/j.expneurol.2018.01.006.

[28] Liu Y, Zhang T, Wang Y et al. Apelin-13 attenuates early brain injury following subarachnoid hemorrhage via suppressing neuronal apoptosis through the GLP-1R/PI3K/Akt signaling. *Biochem Bioph Res Co*, 2019; 513: 105-111. DOI: 10.1016/j.bbrc.2019.03.151.

[29] Luo H, Xiang Y, Qu X et al. Apelin-13 suppresses neuro-inflammation against cognitive deficit in a streptozotocin-induced rat model of alzheimer's disease through activation of BDNF-TrkB signaling pathway. *Front Pharmacol*, 2019; 10: 395. DOI: 10.3389/fphar.2019.00395.

[30] Huang C, Dai C, Gong K et al. Apelin-13 protects neurovascular unit against ischemic injuries through the effects of vascular endothelial growth factor. *Neuropeptides*, 2016; 60: 67-74. DOI: 10.1016/j.npep.2016.08.006.

[31] Ishimaru Y, Sumino A, Kajioka D et al. Apelin protects against NMDA-induced retinal neuronal death via an APJ receptor by activating Akt and ERK1/2, and suppressing TNF-alpha expression in mice. *J Pharmacol Sci*, 2017; 133: 34-41. DOI: 10.1016/j.jphs.2016.12.002.

[32] Zhao Y, Xin Z, Li N et al. Nano-liposomes of lycopene reduces ischemic brain damage in rodents by regulating iron metabolism. *Free Radic Biol Med*, 2018; 124: 1-11. DOI: 10.1016/j.freeradbiomed.2018.05.082.

[33] Turjeman K, Bavli Y, Kizelsztein P et al. Nano-Drugs based on nano sterically stabilized liposomes for the treatment of inflammatory neurodegenerative diseases. *PLoS One*, 2015; 10: e0130442. DOI: 10.1371/journal.pone.0130442.

[34] Pilakka-Kanthikeel S, Atluri VSR, Sagar V et al. Targeted brain derived neurotropic factors (BDNF) delivery across the blood-brain barrier for neuro-protection using magnetic nano carriers: an in-vitro study. *PLoS One*, 2013; 8: e62241. DOI: 10.1371/journal.pone.0062241.

[35] Zhang CJ, Jiang M, Zhou H et al. TLR-stimulated IRAKM activates caspase-8 inflammasome in microglia and promotes

neuroinflammation. *J Clin Invest*, 2018; 128: 5399-412. DOI: 10.1172/JCI121901.

[36] Galatro TF, Holtman IR, Lerario AM et al. Transcriptomic analysis of purified human cortical microglia reveals age-associated changes. *Nat Neurosci*, 2017; 20: 1162-71. DOI: 10.1038/nn.4597.

[37] Shi H, Hua X, Kong D et al. Role of Toll-like receptor mediated signaling in traumatic brain injury. *Neuropharmacology*, 2019; 145: 259-67. DOI: 10.1016/j.neuropharm. 2018.07.022.

[38] Lou B, De Beuckelaer A, Boonstra E et al. Modular core-shell polymeric nanoparticles mimicking viral structures for vaccination. *J Control Release*, 2019; 293: 48-62. DOI: 10.1016/j.jconrel.2018.11.006.

[39] Wang G, Guo Z, Tong L et al. TLR7 (Toll-Like Receptor 7) facilitates heme scavenging through the BTK (bruton tyrosine kinase)-CRT (calreticulin)-LRP1 (low-density lipoprotein receptor-related protein-1)-Hx (hemopexin) pathway in murine intracerebral hemorrhage. *Stroke*, 2018; 49: 3020-9. DOI: 10.1161/STROKEAHA.118.022155.

[40] Pandey GN, Rizavi HS, Bhaumik R et al. Innate immunity in the postmortem brain of depressed and suicide subjects: Role of Toll-like receptors. *Brain Behav Immun*, 2019; 75: 101-111. DOI: 10.1016/j.bbi.2018.09.024.

[41] Huang SW, Lee YP, Hung YT et al. Exogenous interleukin-6, interleukin-13, and interferon-gamma provoke pulmonary abnormality with mild edema in enterovirus 71-infected mice. *Respir Res*, 2011; 12: 1-9. DOI: 10.1186/1465-9921-12-147.

[42] Zhu L, Yin H, Qian T et al. Distinct expression and clinical value of aquaporin 4 in children with hand, foot and mouth disease caused by enterovirus 71. *J Med Virol*, 2022; 94: 587-593. DOI: 10.1002/jmv.25475.